

Stochastic Effects on the Isothermal Explosion Arising in the Oxidation of Iron (II) by Nitric Acid

F. Mauricio¹ and S. Velasco²

Received October 30, 1985

The oxidation of ferrous ion by nitric acid provides us with an example of an isothermal chemical explosion. We propose a chemical scheme with only two independent variables capable of explaining the explosive behavior, and examine the behavior of the fluctuations during the explosion period. The analysis is based on the numerical integration of the time evolution equations corresponding to the first and the second moments of the probability distribution of the number of particles of Fe^{2+} and HNO_2 . During the time interval of explosion the fluctuations present a peak whose maximum value increases as the volume of the system decreases. Comparison with the results of deterministic analysis is performed.

KEY WORDS: Chemical explosion; stochastic analysis; nonlinear phenomena.

1. INTRODUCTION

Epstein *et al.*⁽¹⁾ have proposed a reaction scheme, based on experimental results obtained by spectrophotometric and potentiometric techniques, for the oxidation of ferrous ion at high nitric acid concentration. In this scheme the chemical system displays an explosive behavior in the form of a slow induction period suddenly interrupted by ignition. The latter is characterized by a sharp increase of the reaction rates, followed by a saturation to a final plateau value.

Recently, some works⁽²⁾⁻⁽⁵⁾ showed the necessity to incorporate fluctuations in the study of the chemical explosion regime. In many instances the strength of the fluctuations is scaled by an inverse power of the particle

¹ Departamento de Física, Universidad de La Laguna, Tenerife, Spain.

² Departamento de Termología, Universidad de Salamanca, 37008 Salamanca, Spain.

number of the system, and their effect is small. However, it has been pointed out that the quick evolution associated to the ignition process may counteract the scaling of the fluctuations which, even for relatively large systems, can attain values comparable to the mean values. Therefore, during the ignition step the system can display chaotic behavior dominated by stochastic effects.

This paper is devoted to the study of the fluctuations associated to the oxidation of ferrous ion by nitric acid during the explosion period. Our analysis is based on a simplified version of the Epstein model, thanks to which the explosive behavior can be treated with a reduced number of variables.

In Section 2, on the basis of the numerical discussion of the full Epstein model, we propose a simplified chemical scheme capable of explaining the explosive behavior. Section 3 is devoted to the deterministic analysis of this model. In Section 4 we obtain information on the importance of the fluctuations by performing a numerical integration of the first and second moment equations associated to the simplified model. Discussion of the results is contained in Section 5.

2. THE MODEL

Epstein's model consists of the seven reactions depicted in Table I. Reactions R1, R2, and R3 describe the reduction of nitrate to nitric oxid by ferrous ion. Reaction R4 describe the formation of the FeNO^{2+} intermediate complex, while reactions R5, R6, and R7 summarize the chemistry of the oxynitrogen species.

With the initial conditions depicted in Table II, Fig. 1 summarizes the numerical integration of the deterministic evolution equations for the concentrations of the chemical species in the model. The graphs presented in this figure show the following features:

- (i) After an induction step, the HNO_2 and NO_2 concentrations increase quickly reaching, in the neighborhood of a critical time $t_c \sim 1440$ s, practically their steady-state levels.
- (ii) The NO concentration increases to reach a peak value around t_c , from which it is suddenly decreased to its steady-state level.
- (iii) The FeNO^{2+} concentration reaches a peak around t_c . The relation

$$[\text{FeNO}^{2+}] = \frac{k_4}{k_{-4}} [\text{Fe}^{2+}][\text{NO}] \quad (2.1)$$

is always fulfilled, and so the FeNO^{2+} complex concentration serves as an indicator for the Fe^{2+} and NO concentrations.

Table I. Epstein's Reaction Scheme^a

Number	Reaction and velocities	Kinetic parameters
R1	$\text{Fe}^{2+} + \text{NO}_3^- + 2\text{H}^+ = \text{Fe}^{3+} + \text{NO}_2 + \text{H}_2\text{O}$ $v_1 = \kappa_1 [\text{Fe}^{2+}] [\text{NO}_3^-]$ $v_{-1} = \kappa_{-1} [\text{Fe}^{3+}] [\text{NO}_2] / [\text{H}^+]^2$	$\kappa_1 = 1.0 \times 10^{-6} M^{-1} s^{-1}$ $\kappa_{-1} = 2.8 \times 10^{-4} Ms^{-1}$
R2	$\text{Fe}^{2+} + \text{NO}_2 + \text{H}^+ = \text{Fe}^{3+} + \text{HNO}_2$ $v_2 = \kappa_2 [\text{Fe}^{2+}] [\text{NO}_2]$ $v_{-2} = \kappa_{-2} [\text{Fe}^{3+}] [\text{HNO}_2] / [\text{H}^+]$	$\kappa_2 = 1.2 \times 10^4 M^{-1} s^{-1}$ $\kappa_{-2} = 2.3 \times 10^{-5} s^{-1}$
R3	$\text{Fe}^{3+} + \text{HNO}_2 + \text{H}^+ = \text{Fe}^{3+} + \text{NO} + \text{H}_2\text{O}$ $v_3 = \left(\kappa_{3a} + \kappa_{3b} [\text{H}^+] + \kappa_{3c} \frac{[\text{HNO}_2]}{[\text{NO}]} \right) [\text{Fe}^{2+}] [\text{HNO}_2]$ $v_{-3} = \left(\kappa_{-3a} \frac{[\text{NO}]}{[\text{H}^+]} + \kappa_{-3b} [\text{NO}] + \kappa_{-3c} \frac{[\text{HNO}_2]}{[\text{H}^+]} \right) [\text{Fe}^{3+}]$	$\kappa_{3a} = 7.8 \times 10^{-3} M^{-1} s^{-1}$ $\kappa_{3b} = 3.4 \times 10^1 M^{-2} s^{-1}$ $\kappa_{3c} = 7.6 \times 10^{-3} M^{-1} s^{-1}$ $\kappa_{-3a} = 1.6 \times 10^{-2} s^{-1}$ $\kappa_{-3b} = 1.6 \times 10^{-2} M^{-1} s^{-1}$ $\kappa_{-3c} = 1.6 \times 10^{-2} s^{-1}$
R4	$\text{Fe}^{2+} + \text{NO} = \text{FeNO}^{2+}$ $v_4 = \kappa_4 [\text{Fe}^{2+}] [\text{NO}]$ $v_{-4} = \kappa_{-4} [\text{FeNO}^{2+}]$	$\kappa_4 = 6.3 \times 10^5 M^{-1} s^{-1}$ $\kappa_{-4} = 1.4 \times 10^3 s^{-1}$
R5	$2\text{NO}_2 + \text{H}_2\text{O} = \text{HNO}_2 + \text{NO}_3^- + \text{H}^+$ $v_5 = \kappa_5 [\text{NO}_2]^2$ $v_{-5} = \kappa_{-5} [\text{HNO}_2] [\text{NO}_3^-] [\text{H}^+]$	$\kappa_5 = 2.3 \times 10^7 M^{-1} s^{-1}$ $\kappa_{-5} = 9.6 \times 10^{-4} M^{-2} s^{-1}$
R6	$2\text{HNO}_2 = \text{NO} + \text{NO}_2 + \text{H}^+$ $v_6 = \kappa_6 [\text{HNO}_2]^2$ $v_{-6} = \kappa_{-6} [\text{NO}] [\text{NO}_2]$	$\kappa_6 = 5.8 M^{-1} s^{-1}$ $\kappa_{-6} = 7.4 \times 10^6 M^{-1} s^{-1}$
R7	$\text{NO} + \text{NO}_3^- + \text{H}^+ = \text{NO}_2 + \text{HNO}_2$ $v_7 = \kappa_7 [\text{NO}_3^-] [\text{NO}] [\text{H}^+]^2$ $v_{-7} = \kappa_{-7} [\text{NO}_2] [\text{HNO}_2] [\text{H}^+]$	$\kappa_7 = 5.0 \times 10^{-2} M^{-3} s^{-1}$ $\kappa_{-7} = 9.7 \times 10^3 M^{-2} s^{-1}$

^a v_n and v_{-n} are, respectively, the forward and reverse rates for the n th reaction.

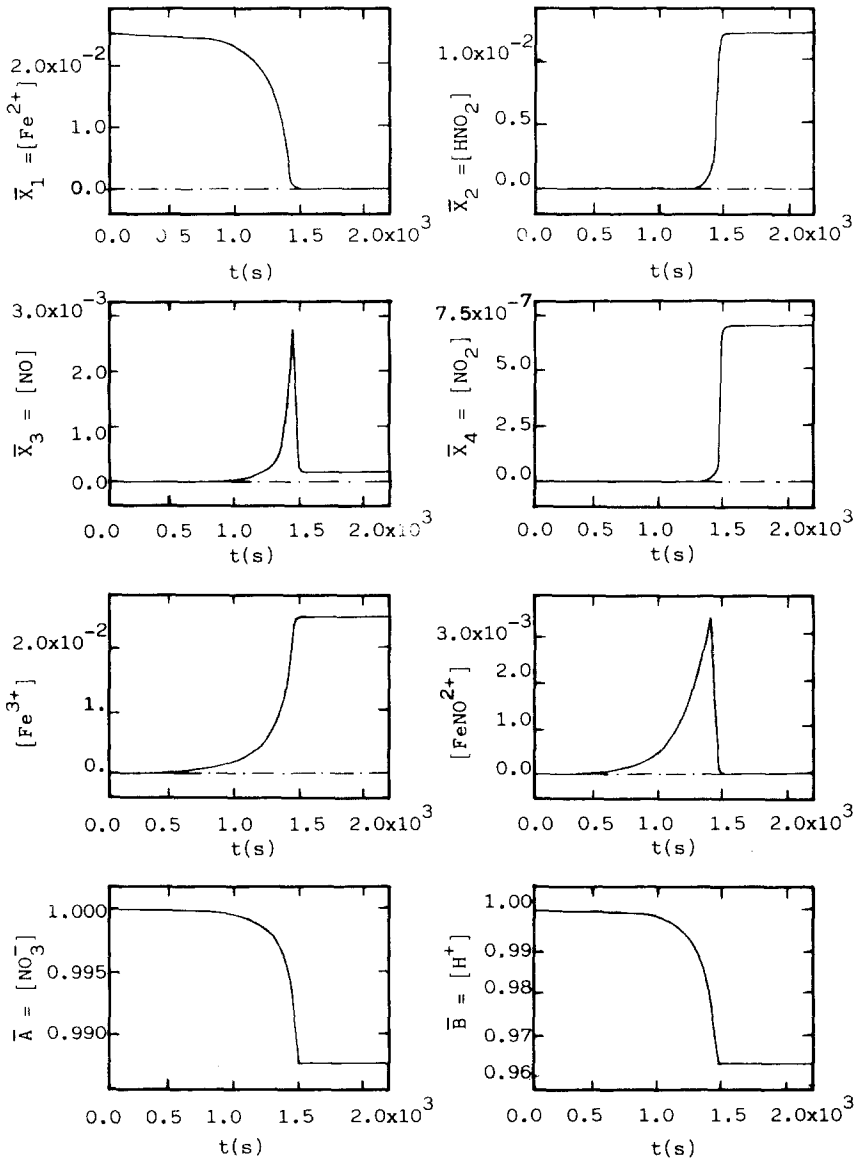


Fig. 1. Time evolution of the chemical specie concentrations obtained from numerical integration of the rate equations associated to Epstein's model (Table I) with initial values depicted in Table II.

Table II. Initial Concentrations Used in the Numerical Integration of Epstein's Model

$[\text{Fe}^{2+}]_o = 0.025M$	$[\text{HNO}_2]_o = 2.0 \times 10^{-6}M^{-1}[\text{H}^+]_o$	$[\text{NO}_3^-]_o = 2.0 \times 10^{-6}M$
$[\text{Fe}^{3+}]_o = 0$		
$[\text{FeNO}^{2+}]_o = 0$	$[\text{NO}_2]_o = \frac{\kappa_{-5}}{\kappa_5} [\text{HNO}_2]_o [\text{H}^+]_o^{1/2} = 9.0 \times 10^{-9}M$	
$[\text{NO}_3^-]_o = 1.0M$		
$[\text{H}^+]_o = 1.0M$	$[\text{NO}]_o = \frac{\kappa_6}{\kappa_{-6}} \frac{[\text{HNO}_2]_o^2}{[\text{NO}_2]_o^2} = 3.5 \times 10^{-10}M$	

- (iv) The Fe^{2+} , NO_3^- , and H^+ concentrations decrease monotonically with a rate which increases quickly in the neighborhood of t_c . The Fe^{3+} concentration shows the inverse behavior.

In order to introduce a simplified model describing this chemical explosion, we have realized, with the initial conditions of Table II, numerical trials in which some of the reactions in Epstein's model were discarded. These led us to the following conclusions for the role of each step:

Reaction R1: The main effect of the forward reaction is to change slightly the explosion time t_c . The effect of the reverse reaction is negligible.

Reaction R2: The forward reaction is negligible and the elimination of the reverse reaction changes the final concentration values slightly.

Reaction R3: The forward reaction is essential to explain the explosion, but the terms with kinetic parameters κ_{3a} and κ_{3c} are negligible for this phenomenon. The reverse reaction only changes the final steady-state values.

Reaction R4: It displaces in a noticeable way the explosion time t_c , but does not influence the explosive behavior.

Reaction R5: This reaction is absolutely negligible in order to explain the explosion.

Reaction R6: The forward reaction is negligible but the reverse reaction is essential to explain the explosion.

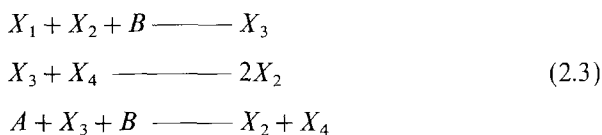
Reaction R7: The forward reaction is essential to explain the explosive behavior and the reverse reaction is negligible.

Therefore, the most simplified set of chemical steps which still provides a description for the explosive behavior must be based on the forward reactions of R3 and R7 and the reverse reaction of R6.

With the notation

$$\begin{aligned}
 X_1 &= \text{Fe}^{2+} & X_2 &= \text{HNO}_2 \\
 X_3 &= \text{NO} & X_4 &= \text{NO}_2 \\
 A &= \text{NO}_3^- & B &= \text{H}^+
 \end{aligned}
 \tag{2.2}$$

we thus adopt the following scheme



Since the NO_3^- and H^+ concentrations greatly exceed that of Fe^{2+} (as is shown in Fig. 1) we shall consider that the concentrations of A (NO_3^-) and B (H^+) remain constant and equal to 1.0 M. With this condition the kinetic parameters of the system (2.3) are

$$\begin{aligned}
 \kappa'_1 = \kappa_{3b} &= 3.4 \times 10^1 M^{-2} \text{s}^{-1} \\
 \kappa'_2 = \kappa_{-6} &= 7.4 \times 10^6 M^{-1} \text{s}^{-1} \\
 \kappa'_3 = \kappa_7 [\text{H}^+] &= 5.0 \times 10^{-2} M^{-2} \text{s}^{-1}
 \end{aligned}
 \tag{2.4}$$

The numerical integration of the rate equations associated to the system (2.3) with the same initial conditions to those imposed to Epstein's model leads to the graphs of Fig. 2. Comparison of Fig. 1 and Fig. 2 shows that the essential difference between our simplified model and the full Epstein model consists in a displacement of the explosion time t_c , i.e., in our model the induction period has been reduced but the explosion itself is essentially described in a similar way.

3. DETERMINISTIC ANALYSIS

The deterministic rate equations for the transient evolution of concentrations in model (2.3) under from nonequilibrium initial conditions, can be written as

$$\begin{aligned}
 \frac{d\bar{x}_1}{d\tau} &= -\bar{x}_1 \bar{x}_2 \\
 \frac{d\bar{x}_2}{d\tau} &= -\bar{x}_1 \bar{x}_2 + 2\bar{x}_3 \bar{x}_4 + \bar{x}_3 \\
 \frac{d\bar{x}_3}{d\tau} &= \bar{x}_1 \bar{x}_2 - \bar{x}_3 \bar{x}_4 - \bar{x}_3 \\
 \frac{d\bar{x}_4}{d\tau} &= \varepsilon^{-1} (-\bar{x}_3 \bar{x}_4 + \bar{x}_3)
 \end{aligned}
 \tag{3.1}$$

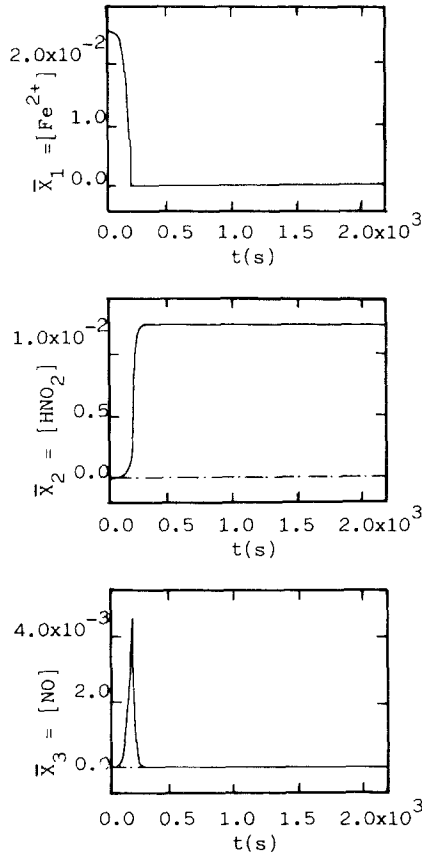


Fig. 2. Solution of the rate equations associated to the chemical scheme (2.3) with kinetic parameters given by (2.4) and the same initial conditions as Epstein's model.

where we have introduced the dimensionless intensive variables $\bar{x}_1, \bar{x}_2, \bar{x}_3,$ and \bar{x}_4

$$\begin{aligned}
 \bar{x}_1 &= \frac{\kappa'_1}{\kappa'_3 \bar{A}} \bar{X}_1 & \bar{x}_2 &= \frac{\kappa'_1}{\kappa'_3 \bar{A}} \bar{X}_2 \\
 \bar{x}_3 &= \frac{\kappa'_1}{\kappa'_3 \bar{A}} \bar{X}_3 & \bar{x}_4 &= \frac{\kappa'_2}{\kappa'_3 \bar{A} \bar{B}} \bar{X}_4
 \end{aligned}
 \tag{3.2}$$

the dimensionless time

$$\tau = \kappa'_3 \bar{A} \bar{B} t
 \tag{3.3}$$

and the dimensionless parameter

$$\varepsilon = \kappa'_1 \bar{B} / \kappa'_2 \quad (3.4)$$

\bar{X}_i , \bar{A} , and \bar{B} are the concentrations of the corresponding chemical species, and t is the time.

We are dealing with a four-variable nonlinear phenomenon whose steady-state will be investigated first.

Taking into account the values of the kinetic parameters κ'_1 and κ'_2 given by (2.4) and that $\bar{B} = 1.0 M$, from (3.4) we have $\varepsilon = 4.6 \times 10^{-6}$. So the system (3.1) involves, in all integration domain, two time scales, i.e., \bar{x}_4 is a quick variable compared to the rest of the variables. Applying Tikhonov's theorem, we can substitute the last differential equation in (3.1) by the algebraic equation

$$-\bar{x}_3 \bar{x}_4 + \bar{x}_3 = 0 \quad (3.5)$$

from which one gets

$$\bar{x}_4 = 1 \quad (3.6)$$

Substitution of (3.6) into (3.1) leads to

$$\begin{aligned} \frac{d\bar{x}_1}{d\tau} &= -\bar{x}_1 \bar{x}_2 \\ \frac{d\bar{x}_2}{d\tau} &= -\bar{x}_1 \bar{x}_2 + 3\bar{x}_3 \\ \frac{d\bar{x}_3}{d\tau} &= \bar{x}_1 \bar{x}_2 - 2\bar{x}_3 \end{aligned} \quad (3.7)$$

Moreover, (3.7) shows that the variables \bar{x}_1 , \bar{x}_2 , and \bar{x}_3 fulfill the relation

$$\frac{d\bar{x}_1}{d\tau} + 2 \frac{d\bar{x}_2}{d\tau} + 3 \frac{d\bar{x}_3}{d\tau} = 0 \quad \text{or} \quad (3.8a)$$

$$\bar{x}_1 + 2\bar{x}_2 + 3\bar{x}_3 = \bar{c} \quad (3.8b)$$

where the constant \bar{c} can be determined from the initial conditions

$$\bar{c} = (\bar{x}_1)_0 + 2(\bar{x}_2)_0 + 3(\bar{x}_3)_0 = (\kappa'_1 / \kappa'_3 \bar{A}) [(\bar{X}_1)_0 + 2(\bar{X}_2)_0 + 3(\bar{X}_3)_0] \quad (3.9)$$

Thus, the system (3.1) contains effectively only two independent variables. If we choose \bar{x}_1 and \bar{x}_2 as such variables, (3.7) becomes

$$\begin{aligned} \frac{d\bar{x}_1}{d\tau} &= -\bar{x}_1\bar{x}_2 \\ \frac{d\bar{x}_2}{d\tau} &= \bar{c} - \bar{x}_1 - 2\bar{x}_2 - \bar{x}_1\bar{x}_2 \end{aligned} \tag{3.10}$$

Equations (3.10) admit two steady-state solutions

$$(\bar{x}_1)_{ss} = 0 \quad (\bar{x}_2)_{ss} = \bar{c}/2 \quad \text{and} \tag{3.11}$$

$$(\bar{x}_1)_{ss} = \bar{c} \quad (\bar{x}_2)_{ss} = 0 \tag{3.12}$$

The linear stability analysis⁽²⁾ leads to the conclusions summarized in Table III for both states: the system possesses only one asymptotically stable steady-state given by the values (3.11).

Figure 3 illustrates graphically the time evolution of the dimensionless variables \bar{x}_1 and \bar{x}_2 to this final stable steady state. They have been obtained by numerical integration of (3.10) with the initial conditions

$$\begin{aligned} (\bar{x}_1)_0 &= 17.0 \\ (\bar{x}_2)_0 &= 1.36 \times 10^{-3} \\ (\bar{x}_3)_0 &= 2.38 \times 10^{-7} \end{aligned} \tag{3.13}$$

which correspond to the initial conditions used in the integration of Epstein's model. In this figure, the scaling of the variables and the time clearly shows the existence, in this simplified model, of an induction period which is essential to give rise to the explosive phenomenon.

Table III. Stationary States of (3.10)^a

Solution	T	Δ	$T^2 - 4\Delta$	Stability	Character	ω_1, ω_2
(3.11)	-	+	+	Stable	Node	Real, negative
(3.12)	-	-	+	Unstable	Saddle	Oposite sign

^a T and Δ are, respectively, the trace and the determinant of the coefficient matrix in the corresponding linearized system. ω_1 and ω_2 are the poles of the characteristic equation.

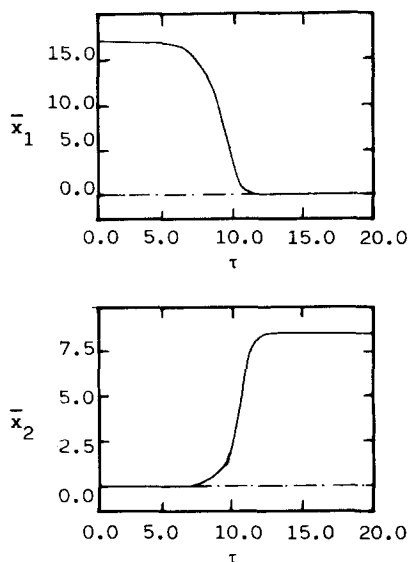


Fig. 3. Solution of (3.10) with initial conditions (3.13).

4. STOCHASTIC ANALYSIS

The phenomenological description shows the existence of a time interval during which the system evolves violently (cf. Fig. 3). It is expected that this phenomenon counteracts the scaling of the fluctuations by the inverse of the size and produces a chaotic regimen dominated by stochastic effects.

In order to study this point, we regard the chemical reactions (2.3) as a birth and death process in the number of particle space.

Like in the deterministic analysis, we assume constant the number density of the particles A and B . Moreover, from (3.8b) and (3.6), we can write for the number of particles X_3 and X_4

$$X_3 = (C - X_1 - 2X_2)/3 \quad (4.1)$$

$$X_4 = N_A V \bar{X}_4 = \frac{\kappa'_3 \bar{A} \bar{B}}{\kappa'_2} N_A V \quad (4.2)$$

where N_A is the Avogadro number, V is the volume, and C is given from the initial conditions

$$C = (X_1)_0 + 2(X_2)_0 + 3(X_3)_0 = N_A V [(\bar{X}_1)_0 + 2(\bar{X}_2)_0 + 3(\bar{X}_3)_0] \quad (4.3)$$

Choosing the number of particles X_1 and X_2 as independent extensive variables, the master equation for the probability distribution $P(X_1, X_2; t)$ of the system (2.3) is

$$\begin{aligned} \frac{dP(X_1, X_2; t)}{dt} &= v_1 B[(X_1 + 1)(X_2 + 1) P(X_1 + 1, X_2 + 1; t) - X_1 X_2 P(X_1, X_2; t)] \\ &\quad + v_2 [X_4(X_3 + 1) P(X_1, X_2 - 2; t) - X_4 X_3 P(X_1, X_2; t)] \\ &\quad + v_3 AB[(X_3 + 1) P(X_1, X_2 - 1; t) - X_3 P(X_1, X_2; t)] \end{aligned} \quad (4.4)$$

where the reaction parameters v_i are related with the kinetic parameters κ'_i by

$$v_1 = \frac{\kappa'_1}{N_A^2 V^2} \quad v_2 = \frac{\kappa'_2}{N_A V} \quad v_3 = \frac{\kappa'_3}{N_A^2 V^2} \quad (4.5)$$

Taking into account (4.1), (4.2), and (4.5), (4.4) becomes

$$\begin{aligned} \frac{dP(X_1, X_2; t)}{dt} &= \lambda(X_1 + 1, X_2 + 1) P(X_1 + 1, X_2 + 1; t) \\ &\quad + \mu(X_1 - 1, X_2 - 1)[P(X_1, X_2 - 1; t) + P(X_1, X_2 - 2; t)] \\ &\quad - [\lambda(X_1, X_2) + 2\mu(X_1, X_2)] P(X_1, X_2; t) \end{aligned} \quad (4.6)$$

where

$$\lambda(X_1, X_2) = v_1 B X_1 X_2 \quad (4.7a)$$

$$\mu(X_1, X_2) = v_3 AB(C - X_1 - 2X_2)/3 \quad (4.7b)$$

From (4.5) and (4.6) the extensive character of these transition rates becomes clear.

In order to investigate the strength of the fluctuations we derive the moment equations.⁽²⁾ From (4.6) we obtain for the first and second moment evolutions

$$\begin{aligned} d\langle X_1 \rangle / dt &= -v_1 B \langle X_1 X_2 \rangle \\ d\langle X_2 \rangle / dt &= v_3 ABC - v_3 AB \langle X_1 \rangle - 2v_3 AB \langle X_2 \rangle - v_1 B \langle X_1 X_2 \rangle \\ d\langle X_1^2 \rangle / dt &= v_1 B \langle X_1 X_2 \rangle - 2v_1 B \langle X_1^2 X_2 \rangle \\ d\langle X_2^2 \rangle / dt &= \frac{1}{3} v_3 AB(C - 3) - \frac{2}{3} v_3 AB \langle X_1 \rangle + 2v_3 AB(C - 2) \langle X_2 \rangle \\ &\quad - 4v_3 AB \langle X_2^2 \rangle + (v_1 B - 2v_3 AB) \langle X_1 X_2 \rangle - 2v_3 \langle X_1 X_2^2 \rangle \\ d\langle X_1 X_2 \rangle / dt &= \frac{1}{3} v_3 AB(3C - 1) \langle X_1 \rangle - v_3 AB \langle X_1^2 \rangle + (v_1 B - 2v_3 AB) \langle X_1 X_2 \rangle \\ &\quad - v_1 B \langle X_1^2 X_2 \rangle - v_1 B \langle X_1 X_2^2 \rangle \end{aligned} \quad (4.8)$$

Let us introduce the dimensionless variables x_1 , x_2 , and τ

$$\begin{aligned}x_1 &= \frac{v_1}{v_3 A} X_1 = \frac{\kappa'_1}{\kappa'_3 \bar{A}} \bar{X}_1 = \bar{x}_1 \\x_2 &= \frac{v_1}{v_3 A} X_2 = \frac{\kappa'_1}{\kappa'_3 \bar{A}} \bar{X}_2 = \bar{x}_2 \\ \tau &= v_3 A B t = \kappa'_3 \bar{A} \bar{B} t\end{aligned}\tag{4.9}$$

and the dimensionless parameters

$$\alpha = \frac{v_1 C}{v_3 A} = \frac{\kappa'_1}{\kappa'_3 \bar{A}} [\bar{X}_1 + 2\bar{X}_2 + 3\bar{X}_3] = \bar{c}\tag{4.10a}$$

$$\beta = \frac{v_1}{v_3 A} = \frac{\kappa'_1}{\kappa'_3 \bar{A}} \frac{1}{N_A V}\tag{4.10b}$$

In terms of x_1 , x_2 , τ , α , and β , the coupled differential equations (4.8) become

$$\begin{aligned}\frac{d\langle x_1 \rangle}{d\tau} &= -\langle x_1 x_2 \rangle \\ \frac{d\langle x_2 \rangle}{d\tau} &= \alpha - \langle x_1 \rangle - 2\langle x_2 \rangle - \langle x_1 x_2 \rangle \\ \frac{d\langle x_1^2 \rangle}{d\tau} &= \beta \langle x_1 x_2 \rangle - 2\langle x_1^2 x_2 \rangle \\ \frac{d\langle x_2^2 \rangle}{d\tau} &= \alpha \beta \left(5 - 3 \frac{\beta}{\alpha} \right) - \frac{5}{3} \beta \langle x_1 \rangle + 2\alpha \left(1 - 2 \frac{\beta}{\alpha} \right) \langle x_2 \rangle \\ &\quad - 4\langle x_2^2 \rangle + 2 \left(\frac{\beta}{2\alpha} - 1 \right) \langle x_1 x_2 \rangle - 2\langle x_1 x_2^2 \rangle \\ \frac{d\langle x_1 x_2 \rangle}{d\tau} &= \frac{\alpha}{3} \left(3 - \frac{\beta}{\alpha} \right) \langle x_1 \rangle - \langle x_1^2 \rangle + 2 \left(\frac{\beta}{2\alpha} - 1 \right) \langle x_1 x_2 \rangle \\ &\quad - \langle x_1^2 x_2 \rangle - \langle x_1 x_2^2 \rangle\end{aligned}\tag{4.11}$$

where the dependence of the evolution on size appears through the volume-dependent parameter β given by (4.10b). In terms of fluctuations

$$\delta x_i = x_i - \langle x_i \rangle \quad (i = 1, 2)\tag{4.12}$$

neglecting the higher than second-order terms in the fluctuations, one can write

$$\begin{aligned} \langle x_i x_j \rangle &= \langle x_i \rangle \langle x_j \rangle + \langle \delta x_i \delta x_j \rangle \\ \langle x_i^2 x_j \rangle &= \langle x_i^2 \rangle \langle x_j \rangle + \langle x_j \rangle \langle \delta x_i^2 \rangle + 2 \langle x_i \rangle \langle \delta x_i \delta x_j \rangle \end{aligned} \tag{4.13}$$

where $i, j = \{1, 2\}$.

Substituting relations (4.12) and (4.13) into (4.11) one gets

$$\begin{aligned} \frac{d\langle x_1 \rangle}{d\tau} &= -\langle x_1 \rangle \langle x_2 \rangle - \langle \delta x_1 \delta x_2 \rangle \\ \frac{d\langle x_2 \rangle}{d\tau} &= \alpha - \langle x_1 \rangle - 2\langle x_2 \rangle - \langle x_1 \rangle \langle x_2 \rangle - \langle \delta x_1 \delta x_2 \rangle \\ \frac{d\langle \delta x_1^2 \rangle}{d\tau} &= \beta \langle x_1 \rangle \langle x_2 \rangle + \beta \langle \delta x_1 \delta x_2 \rangle - 2\langle x_2 \rangle \langle \delta x_1^2 \rangle - 2\langle x_1 \rangle \langle \delta x_1 \delta x_2 \rangle \\ \frac{d\langle \delta x_2^2 \rangle}{d\tau} &= \alpha \beta \left(5 - 3 \frac{\beta}{\alpha} \right) - \frac{5}{3} \beta \langle x_1 \rangle - 4\beta \langle x_2 \rangle + \frac{\beta}{\alpha} \langle x_1 \rangle \langle x_2 \rangle - 4\langle \delta x_2^2 \rangle \\ &\quad + 2 \left(\frac{\beta}{2\alpha} - 1 \right) \langle \delta x_1 \delta x_2 \rangle - 2\langle x_1 \rangle \langle \delta x_2^2 \rangle - 2\langle x_2 \rangle \langle \delta x_1^2 \rangle \\ \frac{d\langle \delta x_1 \delta x_2 \rangle}{d\tau} &= -\frac{\beta}{3} \langle x_1 \rangle + \frac{2\beta}{\alpha} \langle x_1 \rangle \langle x_2 \rangle - \langle \delta x_1^2 \rangle + 2 \left(\frac{\beta}{2\alpha} - 1 \right) \langle \delta x_1 \delta x_2 \rangle \\ &\quad - \langle x_1 \rangle \langle \delta x_2^2 \rangle - \langle x_1 \rangle \langle \delta x_1 \delta x_2 \rangle - \langle x_2 \rangle \langle \delta x_1 \delta x_2 \rangle \end{aligned} \tag{4.14}$$

Figure 4 summarizes the numerical integration of (4.14) for a volume $V = 10^{-9} \text{ cm}^3$ and the initial conditions (3.13) for $\langle x_1(0) \rangle$ and $\langle x_2(0) \rangle$, and $\langle \delta x_i(0) \delta x_j(0) \rangle = 0$ with $i, j = \{1, 2\}$.

By fixing the kinetic parameters and the initial concentrations the role of the fluctuations during the explosion can be linked to the size of the system. Figure 5 shows the time variation of the second-order variances $\langle \delta x_i^2 \rangle^{1/2}$ ($i = 1, 2$) for three values of the volume. One can see that, within the explosion time interval, the variances present a peak whose maximum value increases as volume decreases. Therefore, for sufficiently small volumes, the fluctuations can attain values comparable to the mean $\langle x_i \rangle$. Specifically, one has

- (i) For volumes greater than 10^{-6} cm^3 in the explosion time interval, the second variances $\langle \delta x_i^2 \rangle^{1/2}$ are negligible compared with the mean values $\langle x_i \rangle$, and the system follows the deterministic evolution.

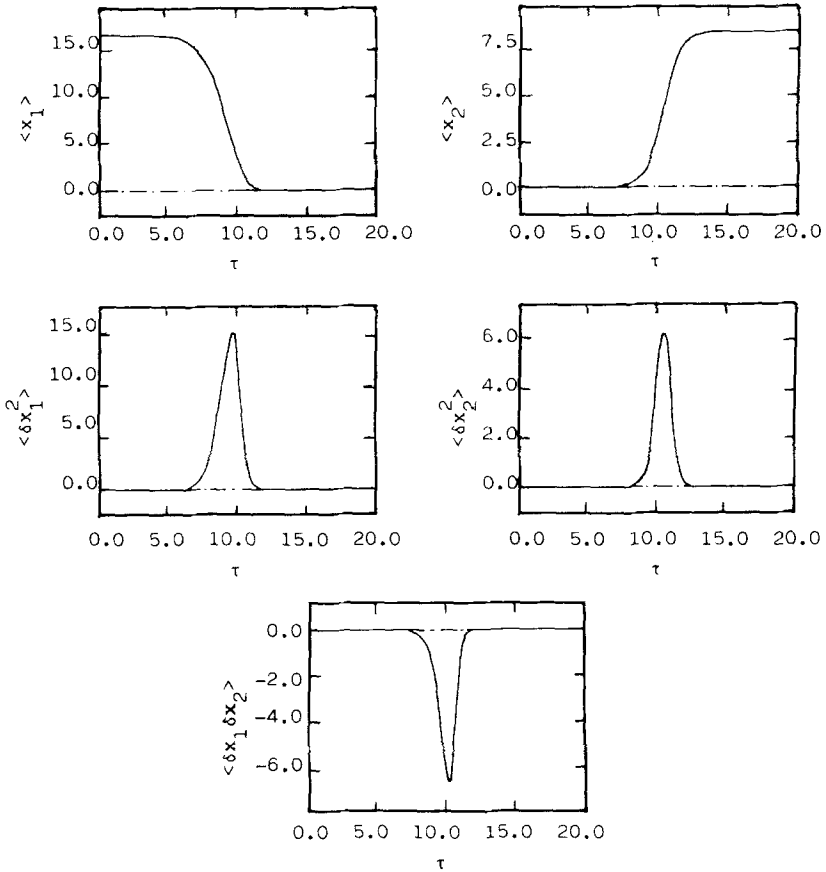


Fig. 4. Solution of (4.14) for a volume $V = 10^{-9} \text{ cm}^3$.

- (ii) For values of the volume from 10^{-6} to 10^{-9} cm^3 , the strength of the fluctuations in the explosion time interval can reach values comparable to the mean but still the functions $\langle x_i(\tau) \rangle$ and $\bar{x}_i(\tau)$ essentially coincide (compare Figs. 3 and 4).
- (iii) When the volume is smaller than 10^{-9} cm^3 , the strength of the fluctuations can be very important during the explosion, and the system exhibits a markedly chaotic behavior.

5. CONCLUSIONS

We have constructed an idealized model which captures the mechanism of the isothermal explosion involved in Epstein's model for the

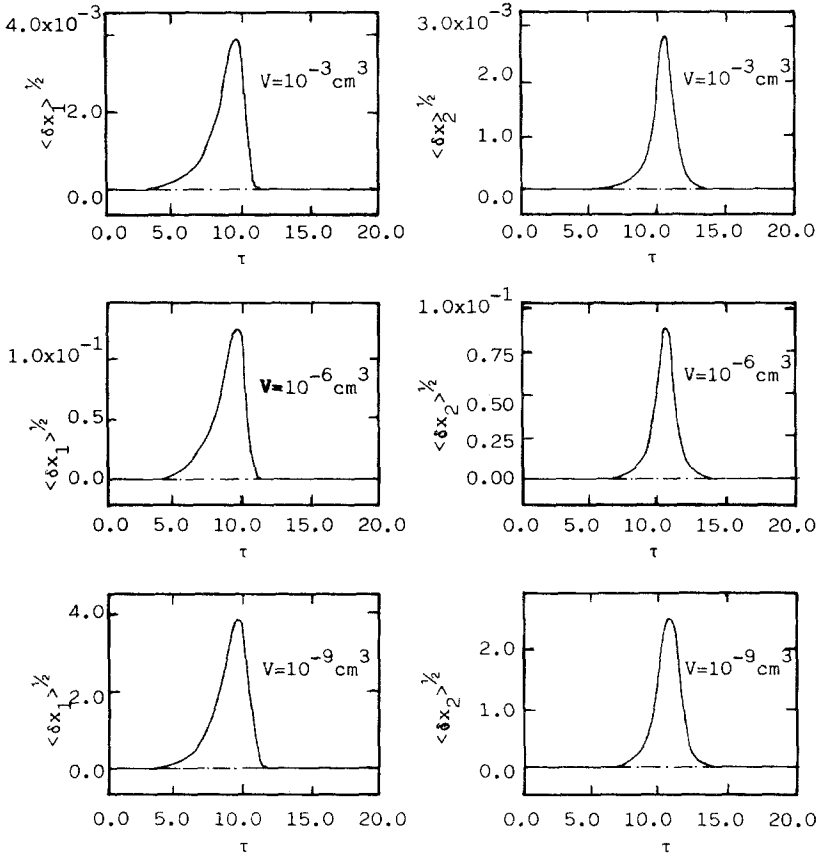


Fig. 5. Time evolution of the second variances $\langle \delta x_1^2 \rangle^{1/2}$ and $\langle \delta x_2^2 \rangle^{1/2}$ obtained from numerical integration of (4.14) for different values of volume V .

oxidation of ferrous ion by nitric acid. This leads to a nonlinear system involving four variables, from which only two turned out to be independent.

The deterministic analysis of the simplified scheme (2.3), with the initial conditions (3.13), shows that after a slow induction period a highly nonlinear and violent evolution appears, during which the system evolves quickly to the unique attractor (3.11).

The stochastic analysis shows that, during the explosion interval, the fluctuations are significantly enhanced. The numerical results establish that, for sufficiently small volumes, such fluctuations become comparable to the mean values. It should be very interesting to try to show experimentally the

existence of these fluctuations. We think that this is feasible if one makes use of laser spectroscopic techniques which can accommodate volumes of the order of those considered in this work ($\sim 10^{-9} \text{ cm}^3$).

ACKNOWLEDGMENTS

We are grateful to Professor G. Nicolis for suggesting this work, and to F. Baras for valuable discussions. We also would like to express thanks for the warm hospitality extended to us by the Department of Chemical Physics II, Free University of Bruxelles, where this work was completed. This research has been supported by the Instituts Internationaux de Physique et de Chimie fondés par E. Solvay.

REFERENCES

1. I. R. Epstein, K. Kustin, and L. J. Warshaw, *J. Am. Chem. Soc.* **102**:3751 (1980).
2. G. Nicolis and I. Prigogine, *Self-Organization in Nonequilibrium Systems* (John Wiley & Sons, New York, 1977).
3. F. Baras, G. Nicolis, M. Malek-Mansour, and J. W. Turner, *J. Stat. Phys.* **32**:1 (1983).
4. M. Frankowicz and G. Nicolis, *J. Stat. Phys.* **33**:595 (1983).
5. G. Nicolis, F. Baras, and M. Malek-Mansour, *Chemical Instabilities*, G. Nicolis and F. Baras, eds. (Reidel Publishers Co., New York, 1984), pp. 171-188.